

The Status of Supersymmetry

Jonathan A. Bagger

*Department of Physics & Astronomy
Johns Hopkins University
Baltimore, MD 21218*

Supersymmetry searches are about to enter an important new era. With LEP 200 and the Main Injector, they will, for the first time, begin to probe significant regions of the supersymmetric parameter space. There is a real chance that supersymmetry might indeed be found before the advent of the LHC.

INTRODUCTION

Up to now, supersymmetry has been a theorist's dream and an experimentalist's nightmare. On the one hand, theorists tend to like supersymmetry because it provides a beautiful mathematical structure which can be used to stabilize the mass hierarchy against radiative corrections. On the other hand, many experimentalists despise the subject because supersymmetric predictions always seem to lie just out of reach.

At present, direct searches for supersymmetry are just shots in the dark because current accelerators do not have the power to explore significant regions of the parameter space. As we will see, this will soon change, but for now, direct searches do not restrict the theory in any important way.

Precision electroweak measurements also reveal very little about supersymmetry. The technical reason for this is that supersymmetry decouples from all standard-model electroweak observables. For example, the supersymmetric and standard-model values of S and T are related as follows (1)

$$\begin{aligned} S_{\text{SUSY}} &= S_{\text{SM}} + \mathcal{O}(M_W/M_S)^2 \\ T_{\text{SUSY}} &= T_{\text{SM}} + \mathcal{O}(M_W/M_S)^2, \end{aligned}$$

where M_W is the mass of the W , and M_S denotes the scale of the supersymmetric spectrum. Theorists can simply raise M_S and bring supersymmetry into complete accord with standard-model predictions.

Fortunately, the next generation of accelerators, including the Fermilab Main Injector, LEP 200, and a possible higher-luminosity Tevatron, will open a new era in supersymmetric particle searches. These accelerators will – for the first time – begin to probe significant regions of the supersymmetric parameter space. And with the advent of the LHC, the search for supersymmetry will finally cover most – if not all – of the parameter space that is relevant for weak-scale supersymmetry.

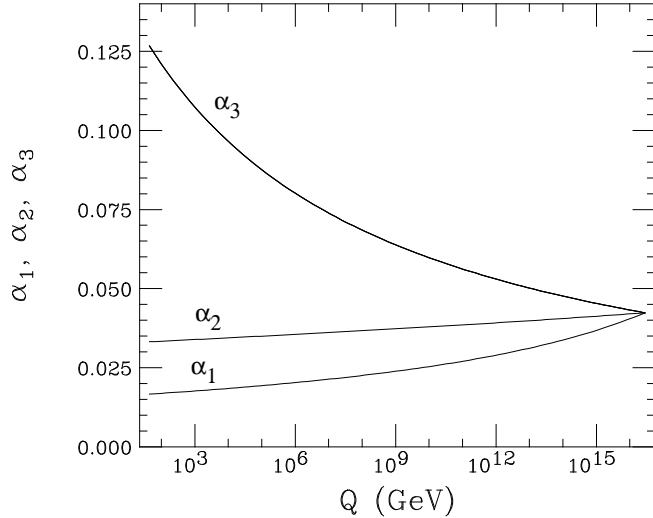


FIG. 1. The gauge couplings unify in the minimal supersymmetric standard model.

In this talk we will examine the supersymmetric parameter space. We will impose supersymmetric unification and show the preferred range for the supersymmetric particle masses. We will also discuss two more specialized points: the constraints on the supersymmetric spectrum that follow from supersymmetric unification, as well as the one-loop constraints on the mass of the lightest Higgs boson.

THE SUPERSYMMETRIC SPECTRUM

Supersymmetry stabilizes the hierarchy $M_W/M_P \simeq 10^{-17}$ against quadratically-divergent radiative corrections. However, it does so at a tremendous cost: a doubling of the particle spectrum. In supersymmetric theories, all bosons are paired with fermions and vice versa. For the case at hand, each of the standard-model particles is accompanied by a supersymmetric partner with the same $SU(3) \times SU(2) \times U(1)$ quantum numbers. If supersymmetry is not broken, these superparticles are degenerate in mass with their original standard-model partners.

The fact that such particles have not been observed tells us that supersymmetry must be broken – and that the breaking must be soft. In other words, the supersymmetry breaking must not reintroduce destabilizing quadratic divergences. The various types of soft supersymmetry breaking have been studied extensively (2). One finds over 50 new parameters:

- 3 gaugino masses: $M_{1/2}^{(a)}$

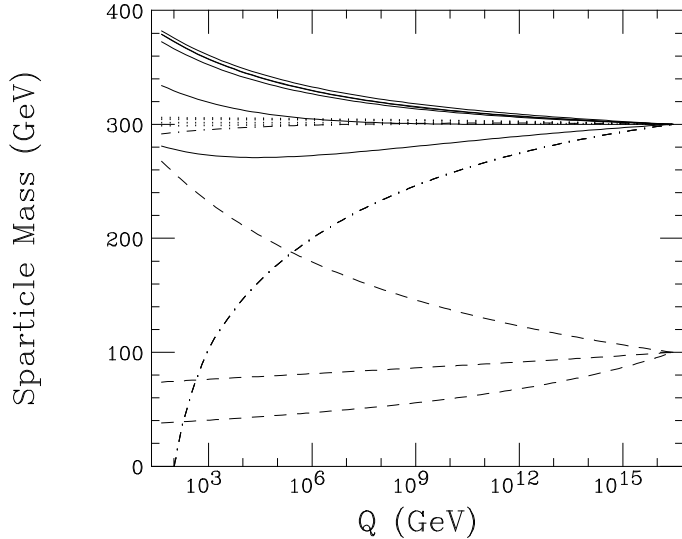


FIG. 2. The soft supersymmetry-breaking masses can be arranged to unify in the supersymmetric standard model. Here $M_0 = 300$ GeV and $M_{1/2} = 100$ GeV. The solid lines denote squark masses and the dotted lines sleptons. The dashed lines are gaugino masses, while the dot-dashed line marks the mass of the Higgs.

- 23 scalar masses: $M_{0\ ij*}^2$
- 27 trilinear scalar couplings: $A_{0\ ijk}$
- 1 bilinear scalar coupling: $B\mu$.

(plus phases). Naturalness requires that each of the dimensionful couplings be less than about a TeV, but that is all we know. The most general softly-broken supersymmetric theory has an enormous parameter space – and theorists are prepared to use every bit of it to evade experimental limits!

Motivated by the successful unification of the gauge couplings in the supersymmetric standard model (Fig. 1), it is not unreasonable to assume that the soft breakings unify as well. In this case the parameter space reduces substantially, to include

- 1 universal gaugino mass: $M_{1/2}$
- 1 universal scalar mass: M_0^2
- 1 universal trilinear scalar coupling: A_0
- 1 bilinear scalar coupling: $B\mu$.

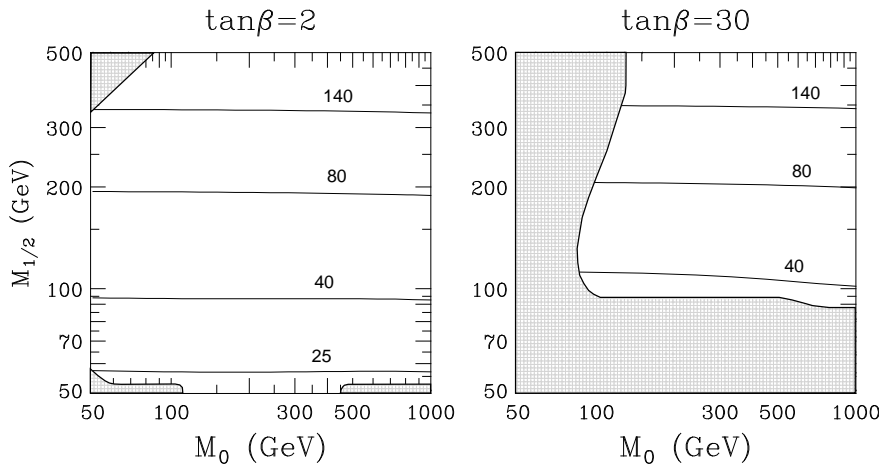


FIG. 3. The mass of the lightest supersymmetric particle, χ_1^0 , for $\mu > 0$, $A_0 = 0$, $\alpha_s(M_Z) = 0.12$ and $M_t = 175$ GeV. The shaded region is forbidden by experimental and theoretical constraints. Most of the supersymmetric parameter space is still open.

As usual in a unified theory, these parameters are fixed at the unification scale M_{GUT} . Their values in the low-energy theory are determined by the renormalization group, as shown in Fig. 2.

At the unification scale, the unification assumption forbids electroweak symmetry breaking because all scalar masses – including that of the Higgs – have the common value M_0^2 . However, top-quark loops decrease the Higgs mass. Therefore, in the renormalization group evolution, they drive down the mass of the Higgs. If the top Yukawa coupling is sufficiently large (corresponding to a top mass of about 150 – 200 GeV), the mass squared goes negative and triggers electroweak symmetry breaking. It is remarkable that this radiative mechanism for symmetry breaking (3), first proposed in 1983, is based on a top-quark mass that is in complete agreement with current experiments!

In what follows, we present expectations for the supersymmetric spectrum based on this unification scenario. For simplicity, we set $A_0 = 0$, and we trade B for the value of $\tan\beta = v_d/v_u$, evaluated at the scale M_Z . In our figures we take $\alpha_s(M_Z) = 0.12$, $M_t = 175$ GeV, and the supersymmetric Higgs mass parameter $\mu > 0$. We find the values of various supersymmetric masses as a function of M_0 and $M_{1/2}$, for two values of $\tan\beta$. (In the figures, all masses are one-loop pole masses.)

In Fig. 3 we show mass contours for the lightest superparticle, χ_1^0 . The χ_1^0 is neutral, and because of a global symmetry called R -parity, is assumed to be stable. In the figure, the shaded areas represent forbidden regions of parameter space, either because of present experimental limits or because of

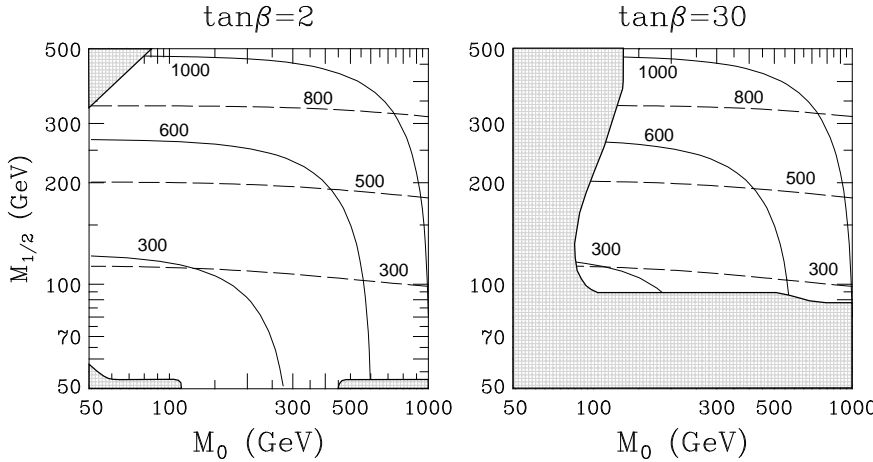


FIG. 4. The mass of the up squark (solid line) and the gluino (dashed line), for $\mu > 0$, $A_0 = 0$, $\alpha_s(M_Z) = 0.12$ and $M_t = 175$ GeV. Our parameter space corresponds to $M_{\tilde{q}} \lesssim 1$ TeV.

theoretical constraints such as the cosmological requirement that the lightest (stable) superparticle be neutral, or the phenomenological constraint that electroweak symmetry be broken, but not color.

In Fig. 4 we show contours for the (up) squark and the gluino masses. (The masses of the up, down, charm and strange squarks are almost degenerate.) From the plot we see that our parameter space covers squark masses up to about 1 TeV. This is the range of interest if supersymmetry is to stabilize the weak-scale hierarchy. (The rule of thumb is that $M_{\tilde{q}} \sim 3M_{1/2}$ and $M_{\tilde{q}}^2 \sim M_0^2 + 4M_{1/2}^2$.)

In Fig. 5 we plot contours for the masses of the lightest Higgs scalar, h , and the lightest chargino, χ_1^\pm . We see that $M_{\chi^\pm} \sim M_{1/2}$, and that for our parameter space, the maximum Higgs mass is about 120 GeV. (For completeness, we note that the slepton masses are approximately $M_{\tilde{\ell}} \sim M_0$.)

Finally, in Fig. 6 we show contours for the lightest stop squark, \tilde{t} , and charged Higgs, H^\pm . From the figure we see that the decays $t \rightarrow \tilde{t}\tilde{\chi}_1^0$ and $t \rightarrow H^\pm b$ are kinematically forbidden over most of the parameter space. (The stop can be lighter for $A_0 \neq 0$, but a very light stop requires a fine tuning of the parameters.)

These figures can be used to illustrate the supersymmetry reach of a given accelerator. For example, LEP 200 has a mass reach of about $\sqrt{s} - 100$ GeV for a supersymmetric Higgs particle, and $\sqrt{s}/2$ for a chargino. Therefore Fig. 5 shows that LEP 200 has an excellent chance of discovering the lightest supersymmetric Higgs and a reasonable possibility of finding the lightest

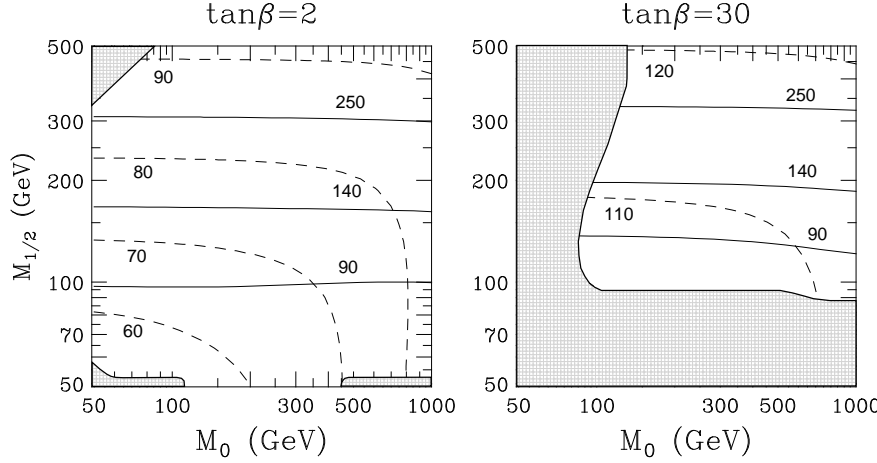


FIG. 5. The mass of the lightest chargino, χ_1^\pm , (solid line) and lightest Higgs, h , (dashed line), for $\mu > 0$, $A_0 = 0$, $\alpha_s(M_Z) = 0.12$ and $M_t = 175$ GeV. The Higgs mass $M_h \lesssim 120$ GeV over our parameter space.

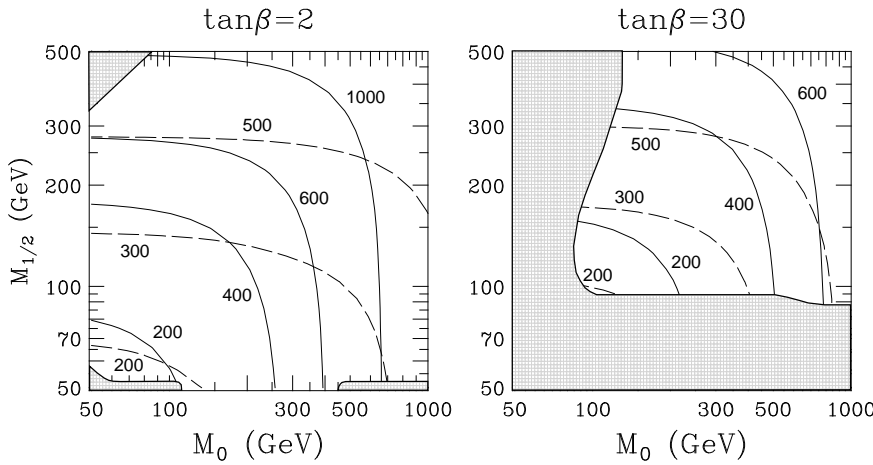


FIG. 6. The mass of the charged Higgs, H^\pm , (solid line) and lightest stop, \tilde{t} , (dashed line), for $\mu > 0$, $A_0 = 0$, $\alpha_s(M_Z) = 0.12$ and $M_t = 175$ GeV. The decays $t \rightarrow \tilde{t}\tilde{\chi}_1^0$ and $t \rightarrow H^+ b$ are kinematically forbidden over most of the parameter space.

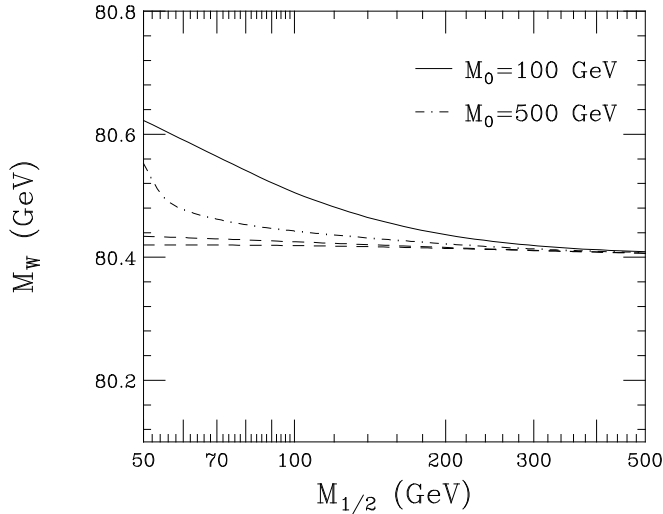


FIG. 7. The one-loop W -boson pole mass, for $\tan\beta = 2$, $A_0 = 0$, $\alpha_s(M_Z) = 0.12$, $M_t = 175$ GeV, and two values of M_0 . The dashed lines correspond to the standard-model W masses, assuming the same Higgs masses as in the supersymmetric cases. Note that the supersymmetry effects decouple for large $M_{1/2}$.

chargino.

The Tevatron's discovery potential is more model-dependent, and varies considerably with the Tevatron luminosity. For an integrated luminosity between 200 pb^{-1} and 25 fb^{-1} , the gluino discovery reach is in the range of $300 - 400$ GeV. Likewise, the chargino/neutralino reach varies between $150 - 250$ GeV in the trilepton decay channel, $\chi_1^+ \chi_2^0 \rightarrow \ell^+ \ell^- \ell'^+$ plus missing energy (4). From Figs. 4 and 5 we see that an upgraded Tevatron would begin to cover a significant amount of the supersymmetric parameter space.

RADIATIVE CORRECTIONS

In the introduction, we argued that precision electroweak measurements cannot be used to restrict the allowed regions of M_0 and $M_{1/2}$ because supersymmetric effects decouple from electroweak observables. This can be seen explicitly in Fig. 7, where we plot the one-loop W -boson pole mass against $M_{1/2}$, for two values of M_0 . We see that the supersymmetric W mass is indistinguishable from the standard-model mass for $M_{1/2} \gtrsim 300$ GeV. The figure also shows that a measurement uncertainty for M_W of 40 MeV gives a sensitivity to the region $M_{1/2} \lesssim 150$ GeV for $M_0 \simeq 100$ GeV. But this is just the region that will be probed directly by LEP 200 and by the Tevatron with the Main Injector!

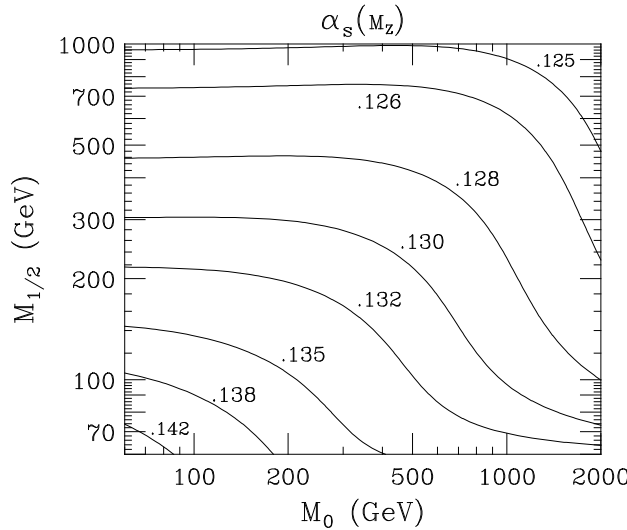


FIG. 8. Contours of $\alpha_s(M_Z)$ in the M_0 , $M_{1/2}$ plane with $m_t = 175$ GeV, $\tan \beta = 2$ and $A_0 = 0$.

In the context of supersymmetric unification, however, precision measurements can play an important role in restricting the supersymmetric parameter space. To see this, we recall that in a unified model, $\alpha_s(M_Z)$ can be predicted as a function of $\alpha_1(M_Z)$, $\alpha_2(M_Z)$, and the weak- and unification-scale thresholds. For the case at hand, we determine $\alpha_1(M_Z)$ and $\alpha_2(M_Z)$ from the electroweak observables α_{EM} , G_F and M_Z . We then calculate the weak-scale thresholds using the minimal supersymmetric standard model, and take the unification-scale thresholds to be those of a particular unified model. In this way we can compute $\alpha_s(M_Z)$ as a function of the parameters M_0 and $M_{1/2}$ in any unified model.

In Fig. 8 we show the prediction for $\alpha_s(M_Z)$ in the absence of unification-scale thresholds. We see that $\alpha_s(M_Z)$ is generally much larger than the experimental value of $\alpha_s(M_Z) = 0.117 \pm 0.005$. Indeed, we see that $\alpha_s(M_Z) \leq 0.127$ requires $M_0 \gtrsim 1$ TeV or $M_{1/2} \gtrsim 500$ GeV (5).

In Fig. 9 we show the effects of unification-scale thresholds. We parametrize these thresholds by ϵ_g , and illustrate the allowed values in the minimal and missing-doublet SU(5) models, together with the threshold required to give $\alpha_s(M_Z) = 0.117 \pm 0.01$. From the figure we see that minimal SU(5) requires $M_0 \gtrsim 1$ TeV, which leads to squark masses of more than 1 TeV.

Weak-scale radiative corrections are also important in determining the Higgs mass. As is well-known, in supersymmetric models the tree-level Higgs mass is determined by gauge couplings, and is bounded from above by M_Z . For heavy top, this value receives significant radiative corrections, and for

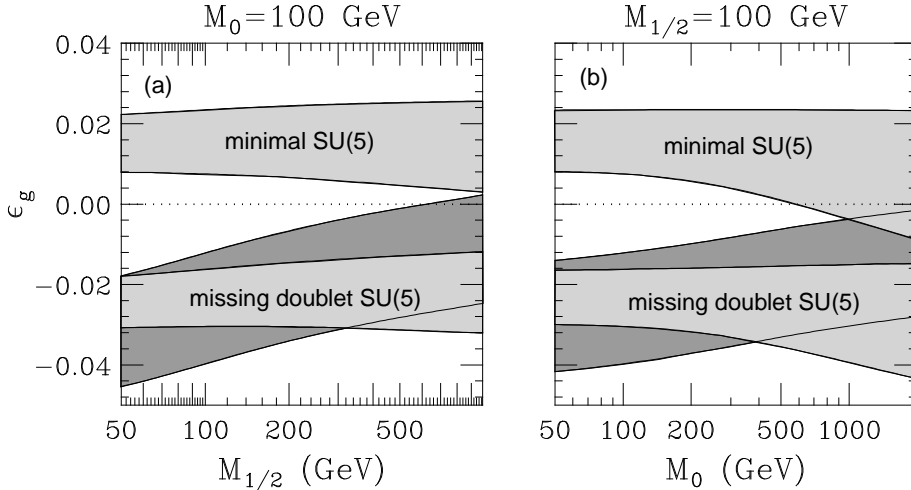


FIG. 9. The light shaded regions indicate the allowed values of the gauge coupling threshold correction ϵ_g in the minimal and missing-doublet SU(5) models. The dark shaded region indicates the range of ϵ_g necessary to obtain $\alpha_s(M_Z) = 0.117 \pm 0.01$.

$M_t \simeq 175$ GeV, the bound increases to about 120 GeV.

Experimentally, this is a very interesting number because it is almost within reach of LEP 200. Theoretically, $M_h \simeq 120$ GeV is interesting as well, because it is approximately the *lower* bound for the Higgs mass in the ordinary, nonsupersymmetric standard model. In the standard model, top-quark loops give a negative logarithmically-divergent ϕ^4 contribution to the effective potential, and this contribution can destabilize the vacuum. If we require that the standard model hold all the way to the Planck scale, so that the cutoff $\Lambda \simeq M_P$, then the Higgs mass must be more than about 120 GeV (6).

This is illustrated in Fig. 10, where we plot the allowed Higgs masses as a function of M_t . From the figure we see that the maximum mass increases with M_t in supersymmetric standard model, as does the minimum mass in the ordinary standard model. The curves have different slopes, and cross at $M_t \simeq 175$ GeV. These curves indicate that if the Higgs is discovered at LEP 200, either supersymmetry is right, or that there must be other new physics below the Planck scale!

CONCLUSIONS

In this talk we have seen that supersymmetry searches are about to enter an important new era. With LEP 200 and the Main Injector, they will begin to probe large regions of the supersymmetric parameter space. With luck,

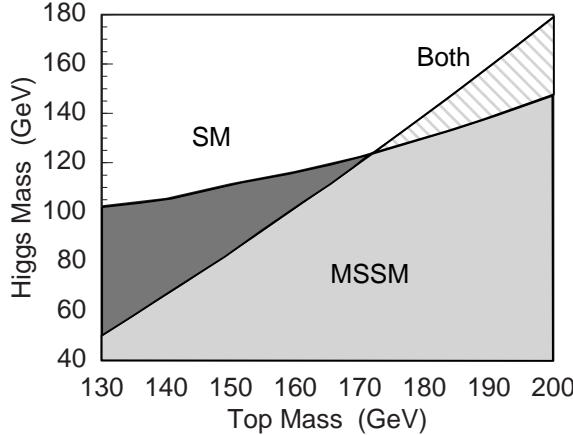


FIG. 10. The maximum one-loop Higgs mass in the minimal supersymmetric standard model, and the minimum Higgs mass in the ordinary standard model, as a function of the top-quark mass (After Ref. (7)).

supersymmetry might even be found before the advent of the LHC!

I would like to thank my collaborators Konstantin Matchev, Renjie Zhang, and especially Damien Pierce for sharing their insights on the supersymmetric standard model. This work was supported by the U.S. National Science Foundation under grant NSF-PHY-9404057.

REFERENCES

1. M. Peskin, T. Takeuchi, Phys. Rev. Lett. **65**, 964 (1990);
D. Kennedy and P. Langacker, Phys. Rev. Lett. **65**, 2967 (1990);
G. Altarelli and R. Barbieri, Phys. Lett. B **253**, 161 (1991).
2. L. Girardello and M. Grisaru, Nucl. Phys. B **194**, 65 (1982).
3. L. Ibañez, Nucl. Phys. B **218**, 514 (1983);
L. Alvarez-Gaumé, J. Polchinski and M. Wise, Nucl. Phys. B **221**, 495 (1983).
4. H. Baer, C. Chen, C. Kao and X. Tata, FSUHEP-HEP-950301;
S. Mrenna, G. Kane, G. Kribs and J. Wells, CIT-68-1986.
5. J. Bagger, K. Matchev, D. Pierce, Phys. Lett. B **348**, 443 (1995).
6. G. Kane, C. Kolda and J. Wells, Phys. Rev. Lett. **70**, 2686 (1993);
J. Espinosa and M. Quiros, Phys. Lett. B **302** 51 (1993);
G. Altarelli and G. Isidori, Phys. Lett. B **337**, 141 (1994);
M. Quiros, in *Physics from the Planck Scale to Electroweak Scale*, eds. P. Nath, T. Taylor and S. Pokorski (World Scientific, 1995);
J. Casas, J. Espinosa and M. Quiros, Phys. Lett. B **342**, 171 (1995).